JOURNAL OF RAMAN SPECTROSCOPY, VOL. 21, 819–825 (1990)

Multiplex Pure Rotational Coherent Anti-Stokes Raman Spectroscopy in a Molecular Beam

Nicolaas Bloembergen, Kuei-Hsien Chen,* Cheng-Zai Lü and Eric Mazur
Gordon McKay Laboratory, Harvard University, Cambridge, Massachusetts 02138, USA

Pure rotational coherent anti-Stokes Raman spectroscopy using a single broad-band dye laser was applied to study the rotational energy distribution of molecules in a pulsed supersonic beam. The multiplex BOXCARS configuration allows the accurate determination of rotational constants and rotational temperatures, and offers many advantages over other methods. The technique was applied to calibrate the cooling effect of a pulsed molecular beam of nitrogen and to study the rotational energy distributions of infrared multiphoton-excited ethylene.

INTRODUCTION

Coherent anti-Stokes Raman spectroscopy (CARS) allows one to probe vibrational and rotational populations of gaseous and liquid samples with high spatial and temporal resolution.[1] For this reason, CARS is widely used in spectroscopy and combustion diagnostics.[1–3] The predominant technique is vibrational CARS and involves a vibrational Raman transition.[4] Pure rotational CARS, which is associated with a rotational Raman transition, is particularly well suited for studying rotational energy distributions, and hence for low-temperature measurements. In the pure rotational case, the line widths are narrower and the Raman cross-sections larger than those for vibrational CARS and the signal intensity is larger.

The energy diagram of pure rotational CARS is shown in Fig. 1. Two lasers of frequency ω_1 and ω_2, with a frequency difference equal to the rotational Raman shift $\omega_R = \omega_1 - \omega_2$, coherently excite a transition between two rotational levels J and J', where J is the rotational quantum number. A third laser at frequency ω_3, which frequently is chosen to be equal to ω_1, scatters off this coherent excitation and generates a CARS signal at a frequency $\omega_c = \omega_3 + \omega_R$. Since rotational Raman shifts are small (<20 cm^{-1}), the laser at the Stokes frequency ω_2 must be tuned close to the laser at frequency ω_1, and a straightforward implementation of this scheme with a single dye laser as in vibrational CARS is impractical. Therefore, pure rotational CARS is typically performed using an excimer laser or the second harmonic of an Nd:YAG laser to pump two closely tuned dye lasers at frequencies ω_1 and ω_2.[5] Alternatively, one can use the third-harmonic of an Nd:YAG laser to pump a coumarin-based dye laser at a frequency ω_2 close to the second harmonic of the Nd:YAG laser at $\omega_1(\omega_2 = \omega_1 - \omega_R)$.[6] In both cases the set-up is more cumbersome than that for vibrational CARS.

The scheme can be significantly simplified, however, by deriving both ω_1 and ω_2 beams from a single broad-band dye laser as shown in Fig. 2. Each rotational transition then selects pairs of photons at frequencies ω_1 and ω_2 within the band width of the broad-band beams,

* Present address: General Electric CRD, P.O. Box 8, Schenectady, NY 12301, USA.

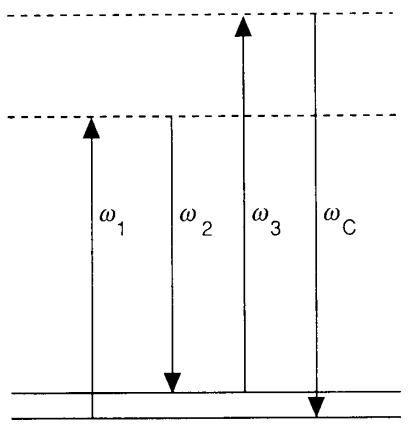

Figure 1. Energy diagram for pure rotational coherent anti-Stokes Raman spectroscopy (CARS)

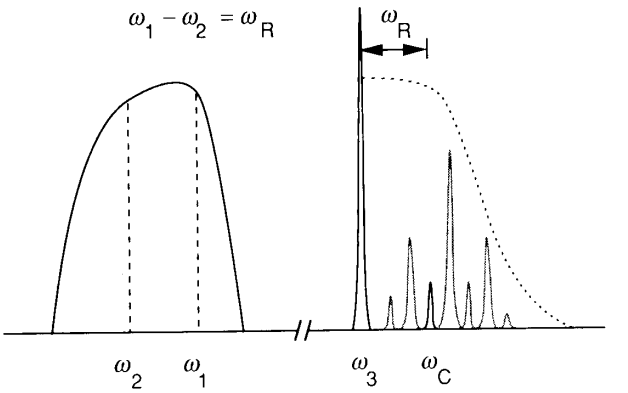

Figure 2. Schematic spectrum of broad-band pure rotational CARS. The two pumping lasers at ω_1 and ω_2 are from a single broad-band dye laser (solid curve, left). This laser provides pairs of photons with a frequency difference corresponding to the rotational Raman transition frequency ω_R. The ω_3 beam is a narrow band laser of arbitrary wavelength. The dashed curve indicates the accessible CARS frequencies that fall within the dye-laser profile.

0377-0486/90/120819-07 $05.00

Received 12 July 1990

such that the frequency difference $\omega_1 - \omega_2$ matches the Raman shift ω_R. Since the rotational constants of molecules are small, a dye laser of band width 60 cm^{-1} easily covers the entire rotational spectrum. Note that the frequency of the laser at ω_3 is not determined by any molecular parameters and may be chosen arbitrarily.

This broad band scheme, introduced by Eckbreth and Anderson,[17] has a number of advantages. First, since a photon at any frequency ω_1 within the band width of the broad-band laser automatically finds a corresponding photon at a frequency ω_2 such that $\omega_1 - \omega_2 = \omega_R$, *all* photons in the broad-band beam are used. This contributes to a stronger CARS signal than in the vibrational scheme where only the resonant frequencies are used.[7] Second, since the center frequency of the broad-band dye laser is arbitrary, one can choose the most efficient dye to improve the signal level. Third, the phase matching is the same for all molecules as long as the rotational Raman spectrum is covered by the broad-band dye laser. Once the beams are properly aligned, therefore, one can switch from one molecule to another without any change in alignment.

To fulfil the phase-matching condition, $k_C = k_1 - k_2 + k_3$, three possibilities exist: colinear, planar crossed-beam and folded BOXCARS.[1,8] In this paper we demonstrate, for the first time, the use of multiplex[9] folded BOXCARS for pure rotational CARS with a single dye laser. The three-dimensional phase-matching geometry is shown in Figs 3(a) and (b). Both k_1 and k_2 are derived from a single broad-band dye laser, k_3 from a narrow-band laser. Note that in this configuration the CARS beam is spatially separated from the pumping beam regardless of the magnitude of the rotational Raman shift. Also, the angle between k_1 and k_2 is much larger than that in the planar case. This avoids the use of a beam-combining dichroic mirror and the use of polarization to suppress the incident laser beams. Moreover, one can easily switch back and forth between vibrational and pure rotational CARS by replacing one of the two broad-band beams with a second narrow-band beam at ω_3. The same broad-band laser can be used for both schemes because the center frequency of the broad-band laser is unimportant for the pure rotational scheme.

In pure rotational CARS spectra one can easily observe Stokes transitions in addition to the anti-Stokes transitions. These transitions, which are at the opposite end of the anti-Stokes transitions with respect to the position of the ω_3 laser beam, are referred to as coherent Stokes Raman spectroscopy (CSRS) lines. The CSRS spectrum is a mirror image of the CARS spectrum.

EXPERIMENTAL

The experimental set-up is shown in Fig. 4. The CARS laser beams are derived from the output of a Quantel YG471C Nd:YAG laser with a 10-ns pulse duration and a 200-mJ average second-harmonic output at 532 nm. An intracavity line-narrowing étalon reduces the line width to 0.05 cm^{-1}. About 50 mJ of the second harmonic is used for the ω_3 beam, while the remainder serves to pump a broad-band dye laser–amplifier system generating the ω_1 and ω_2 beams. The prism-tuned broad-band dye laser, operating on Fluorescein 548 dye around 550 nm, produces 2-mJ pulses of 6-ns pulse duration and 60-cm^{-1} line width. These pulses are amplified to 30 mJ in two stages. All beams are vertically polarized, and are aligned parallel to one another before being focused into the sample with a 30-cm focal length lens. The beam waist and the interaction length of the CARS beams are 80 and 200 μm, respectively.

The CARS beam generated in the interaction region passes through an aperture which spatially rejects the incident beams as shown in Fig. 4. The signal is then dispersed using a Jarrel Ash 78-420 1-m *f*/6.2 monochromator with a 0.05 Å resolution in second order. Instead of using the output slit of the monochromator, the dispersed CARS signal is recorded on the (horizontal) entrance slit of a Hamamatsu C1587 streak camera system with a 512 × 512 detector array. The resulting spectral resolution of the entire system is 0.12 Å. The dispersion of the monochromator was calibrated with the 6-Å separation of the two Na D lines. For each spectrum an average over 50 laser shots is taken to obtain a good signal-to-noise ratio.

Experiments were done in bulk samples and in a supersonic molecular beam. In both cases the sample molecules can be excited by a third laser. In a later section we report on the infrared multiphoton excitation[10–12] of ethylene with a carbon dioxide laser. For that purpose the molecules were irradiated with a 250-ns pulse from a grating-tuned TEA carbon dioxide

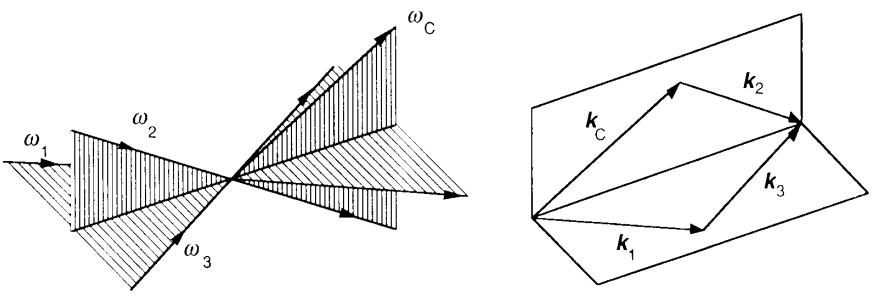

Figure 3. (a) Laser beam configuration for pure rotational CARS. (b) Phase-matching diagram for pure rotational CARS.

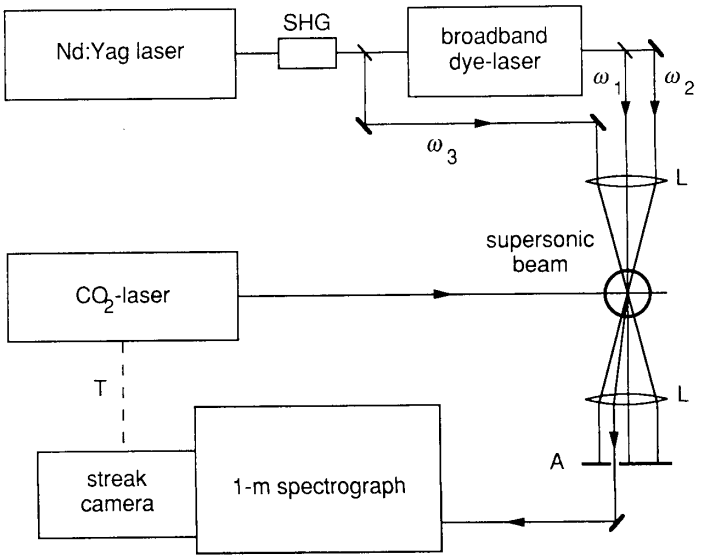

Figure 4. Experimental set-up. SHG = second harmonic generation; L = lens; A = aperture; T = optional streak camera trigger for time-resolved studies.

laser operating on the 10P(14) line. The infrared beam is focused by a cylindrical lens in such a way as to overlap the focal region with the CARS interaction region. The time evolution of the data can be obtained by triggering the streak camera from the exciting laser pulse and using the time resolution of the camera to obtain three-dimensional information of intensity versus wavelength and time.[13]

The pulsed supersonic molecular beam apparatus consists of a nozzle mounted on a translational manipulator and a high vacuum chamber. The nozzle is a Toyota cold-start fuel injector (Model 23260-79055), which has been modified by machining off the fuel injection nozzle to a thickness of about 2 mm. The diameter D of the output aperture is 0.9 mm, and the pressure in the reservoir is between 1 and 3 atm. The nozzle is driven by a custom-built electronic driver at a rate of 10 Hz with a variable opening time of 0.1–1 ms. The chamber is pumped by an Edwards E2M12 rotary pump and an Edwards MK2 700 l s^{-1} diffusion pump. With the molecular beam off, the beam chamber pressure is 4×10^{-7} Torr; with a reservoir pressure of about 3 atm and 1-ms molecular pulses at a 10-Hz repetition rate, the chamber pressure rises to 7×10^{-4} Torr. The beam expands vertically downward into the high-vacuum chamber, which has four windows allowing laser excitation and CARS probing of the molecules in the beam. An XYZ translational manipulator allows one to overlap the molecular beam with the laser beams and to adjust the distance x between the nozzle and the interaction region.

PURE ROTATIONAL CARS OF NITROGEN IN A MOLECULAR BEAM

The pure rotational CARS technique is ideally suited to measure the density and the rotational temperature profiles in the supersonic beam. The rotational CARS frequency shifts for a rigid linear molecule ($\Delta J = 2$) are given by

$$\Delta\omega = B(J + 2)(J + 3) - BJ(J + 1) = 6B + 4BJ \quad (1)$$

where B is the rotational constant. The pure rotational CARS spectrum of nitrogen at room temperature is shown in Fig. 5. The peaks are separated by 8 cm^{-1}, in excellent agreement with the rotational constant B for nitrogen. Note that for rotational Raman shifts much larger than the band width of the broad-band dye laser the signal falls off.

It is important to note that the rotational CARS signal, like vibrational CARS, is determined by the resonant contribution of all rotational transitions to the third-order non-linear susceptibility $\chi^{(3)}$, and is proportional to the square of the population difference between the initial and final rotational states involved in the Raman transition.[14] For the intensity I_J corresponding to a rotational transition from initial state J,

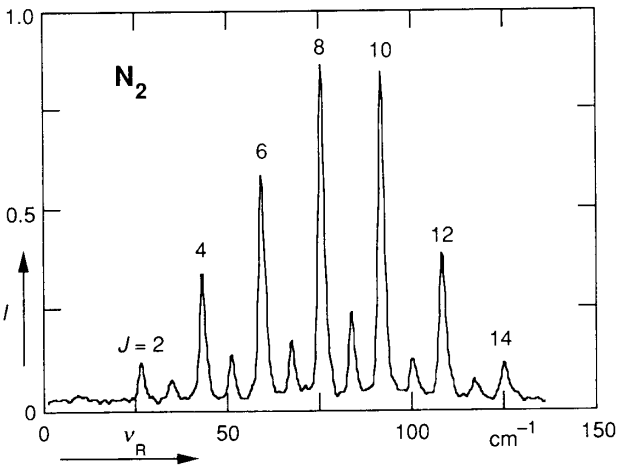

Figure 5. Pure rotational CARS spectrum of nitrogen at room temperature. J indicates the rotational quantum number of the initial Raman transition. Because the populations of even and odd J states have a nuclear spin weight ratio of 2, the spectrum shows an alternating intensity distribution. The vertical scale is arbitrary.

one obtains[8]

$$I_J \propto \left\{\frac{d\sigma(J)}{d\Omega}\frac{Ng_J(2J+1)}{Z_R}\left[e^{-J(J+1)B/kT} - e^{-(J+2)(J+3)B/kT}\right]\right\} \equiv \left\{\frac{d\sigma(J)}{d\Omega}\Delta N_J\right\}^2 \quad (2)$$

where $d\sigma(J)/d\Omega$ is the Raman transition cross-section,[15] N is the number density of the molecules, g_J the nuclear spin weight of the initial state and Z_R the rotational partition function. Equation (2) can be used to evaluate the rotational temperature of the molecules from measured pure rotational spectra such as that shown in Fig. 5.

The translational temperature of the sample is greatly reduced by the adiabatic expansion in the supersonic molecular beam. As the distance x from the nozzle increases, the isentropic temperature of molecules, T_i, decreases according to[16]

$$T_i = \frac{T_0}{1 + \frac{1}{2}(\gamma - 1)M^2} \quad (3)$$

where T_0 is the reservoir temperature, γ the specific heat ratio and M the Mach number, which can be obtained from an empirical relationship[16]

$$M = A\left(\frac{x - x_0}{D}\right)^{\gamma - 1} - \tfrac{1}{2}A^{-1}\frac{\gamma + 1}{\gamma - 1}\left(\frac{x - x_0}{D}\right)^{1-\gamma} \quad (4)$$

The constants A and x_0 depend only on the specific-heat ratio γ. Values for these constants can be found in the literature.[17]

The adiabatic expansion cools not only the translational degrees of freedom but also, indirectly, via collisions, the vibrational and rotational degrees of freedom. Collisions near the nozzle equilibrate the vibrational and rotational temperatures with the translational temperature. As the gas expands, however, the collision rate decreases and the transfer of energy between the various degrees of freedom slows. Generally, the translation–rotation relaxation rate is much higher than the translation–vibration relaxation rate. Therefore the rotational temperature is usually lower than the vibrational temperature, and both are higher than the translational temperature.[18]

Together with this decrease in temperature, one has a decrease in sample pressure p:[16]

$$p = p_0\left(\frac{T_i}{T_0}\right)^{1/(1-\gamma)} \quad (5)$$

As can be seen in Eqn (2), the CARS signal is proportional to the square of the number density N. Consequently, the CARS signal will fall off rapidly when the distance x to the nozzle is increased.

The dramatic cooling of the rotational degree of freedom is evident from the spectra shown in Figs 6 and 7. At a distance $x/D = 5.2$ from the nozzle (see Fig. 6), only states with $J \leqslant 4$ are populated. From a fit to a theoretical spectrum according to Eqn (2), one finds a rotational temperature of 30 K. This is identical with the isentropic temperature one obtains for nitrogen from Eqn (3) at $x/D = 5.2$, indicating a very efficient rotational cooling. Still further away from the nozzle, at $x/D = 11.6$, the isentropic temperature according to Eqn (3) is 15 K. In the measured spectrum only states

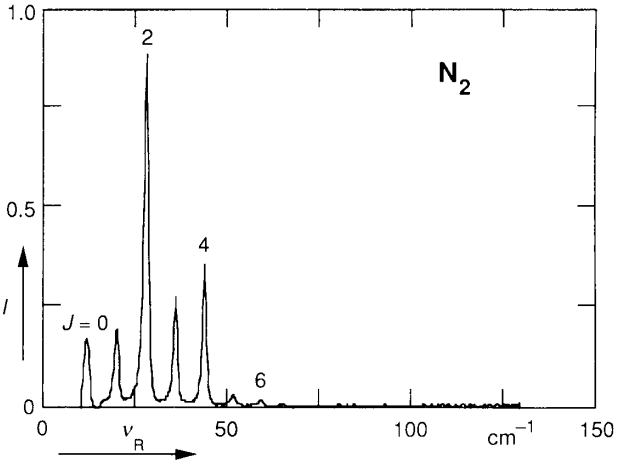

Figure 6. Pure rotational CARS spectrum of nitrogen in a pulsed supersonic beam at $x/D = 5.2$. This spectrum corresponds to a rotational temperature of 30 K.

with $J \leqslant 2$ appear (see Fig. 7). The agreement between this spectrum and Eqn (2), however, is no longer very good. This is probably due to different cooling rates for the *ortho* and *para* modifications of nitrogen.[19]

The density in the supersonic jet can be determined by comparing the pure rotational CARS spectra from molecules in the beam with those obtained in the bulk. According to Eqn (2), the square root of the intensity of each peak in the spectrum corresponding to a certain J value is proportional to the population difference ΔN_J between the J and $J + 2$ states, so that:

$$\Delta N_J = c\left(\frac{d\sigma(J)}{d\Omega}\right)^{-1}\sqrt{I_J} \quad (6)$$

where c is a proportionality constant which depends on the alignment. The total number density of the molecules is then given by

$$N = \sum N_i = \Delta N_0 + \Delta N_1 + 2\Delta N_2 + 2\Delta N_3 + 3\Delta N_4 + 3N_5 + \cdots \quad (7)$$

If one switches between bulk samples and molecular beam without a change in alignment or detector gain, the proportionality constant c remains unchanged. This

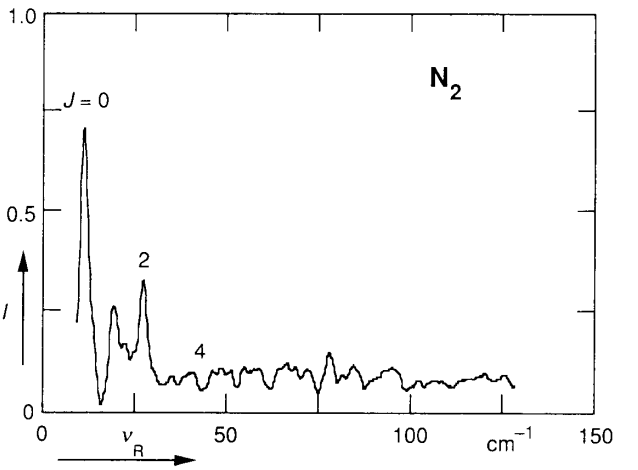

Figure 7. Pure rotational CARS spectrum of nitrogen in a pulsed supersonic beam at $x/D = 11.6$.

allows one to determine the density by comparing the cN obtained from spectra taken in the beam with the value following from bulk measurements at a known pressure and temperature. Note that one must first determine the temperature to correct for the temperature dependence of the partition function. For nitrogen at $x/D = 4.5$ one thus finds for the density in the jet a value of 6×10^{23} m^{-3}.

Because of the high spatial resolution of the BOXCARS configuration, one can map out the entire three-dimensional temperature and density profiles of the expanding beam using this technique. This allows one to characterize completely the flow and optimize the nozzle design. The results also clearly show that the technique yields excellent signal-to-noise ratios even at very small (<5 cm^{-1}) Raman shift and extremely low densities.

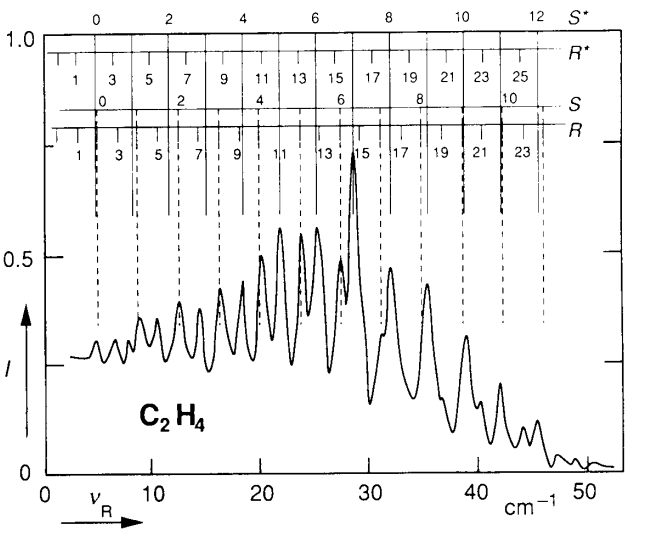

Figure 8. Pure rotational CARS spectrum of ethylene in the bulk at room temperature and 30 Torr. The assignments of *S*, *R*, *S** and *R** branches are described in Table 1.

PURE ROTATIONAL CARS OF INFRARED MULTIPHOTON-EXCITED ETHYLENE

Ethylene is a nearly symmetric asymmetric top molecule. In general, the rotational Raman spectra of asymmetric top molecules are difficult to analyze because of the many rotational degrees of freedom that cause large numbers of overlapping lines to appear in the spectrum. The selection rules for rotational Raman transitions of symmetric top molecules are[20]

$$\Delta J = 0, \pm 1, \pm 2, \Delta K = 0 \qquad (8)$$

where J and K are the rotational quantum numbers corresponding to the angular momentum vector **J** and its projection on the figure axis of the molecule.

Ethylene has three rotational degrees of freedom. The rotation along the C=C axis has the largest rotational constant, but a small Raman cross-section.[20] The other two rotational degrees of freedom have nearly identical rotational constants, making it difficult to resolve the spectrum by conventional Raman spectroscopy.[21] There are four branches in the rotational Stokes spectrum, as listed in Table 1.[21]

The pure rotational CARS spectrum of ethylene in the bulk at room temperature is shown in Fig. 8. The individual lines are clearly resolved and can be assigned to the four branches listed in Table 1. By blocking the strong laser background at zero Raman shift using a thin wire placed in front of the detector array, one can easily observe both CARS and CSRS spectra. Figure 9 shows such a spectrum for ethylene after expansion in the supersonic beam at $x/D = 5.7$. As can be seen, the rotational distribution of ethylene now peaks at much lower J values. The spectrum becomes easier to assign because one can directly compare the Stokes and anti-Stokes lines instead of using the (estimated) position of the laser frequency to determine the Raman shifts. This allows one to determine the rotational constants for ethylene in a straightforward fashion.

The rotational constants obtained from the spectra in Figs 8 and 9 are $\bar{B} = \frac{1}{2}(B + C) = 0.92 \pm 0.01$ cm^{-1} and $C = 0.83 \pm 0.01$ cm^{-1}. For planar molecules the moments of inertia I about the three principal axes of

Table 1. Assignment of the four branches in the rotational Raman spectrum of ethylene

Branch	Transition	Remarks
R	$\Delta J = 1$	Symmetric top part
S	$\Delta J = 2$	Symmetric top part
*R**	$\Delta J = 1$	Contribution of deviation from symmetric top
*S**	$\Delta J = 2$	Contribution of deviation from symmetric top

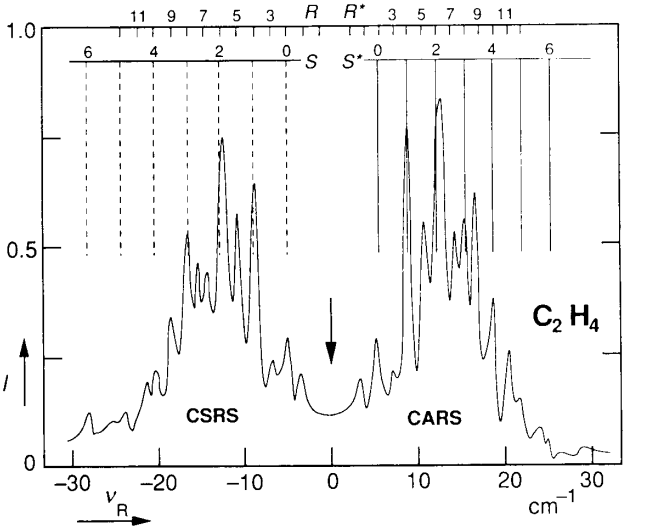

Figure 9. Pure rotational CARS and CSRS spectrum of ethylene in the beam at $x/D = 5.7$. The arrow indicates the position of the incident laser at ω_3. This wavelength was physically blocked out in front of the detector array by a thin wire. Notice that all four *S*, *R*, *S** and *R** branches appear in each of the CARS and CSRS spectra. For simplicity, only the *S* and *R* branches are assigned on the CSRS side, while the *S** and *R** branches are assigned on the CARS side.

Table 2. Comparison of the obtained ethylene rotational constants with published values

Ref.	A (cm^{-1})	B (cm^{-1})	C (cm^{-1})
This work	4.66 ± 0.02	1.01 ± 0.01	0.83 ± 0.01
21	4.828	1.0012	0.8282
20	4.66 ± 0.20	1.008 ± 0.006	0.828 ± 0.003

rotation satisfy the relationship

$$I_C = I_A + I_B \tag{9}$$

where the subscript A labels the figure axis. The rotational constants are related to the moments of inertia by

$$A_i = \frac{h}{8\pi^2 c I_{A_i}} \quad (A_i = A, B, C) \tag{10}$$

Equations (9) and (10) allow one to determine the three rotational constants from the values of $\tilde{B}$ and C. The resulting values listed in Table 2 are in excellent agreement with published values.

To study the effect of infrared excitation on the rotational spectrum, the ν_7 mode of the ethylene molecules was pumped with the 10P(14) carbon dioxide laser line. The result is shown in Fig. 10, where the dashed line is the rotationcal CARS spectrum of ethylene without infrared pumping and the solid line is the spectrum 250 ns after an infrared pulse of 6.3 J cm^{-2}. The lines corresponding to the $J = 1$ and $J = 2$ states are strongly reduced in intensity by the carbon dioxide laser, indicating a depletion of the corresponding rotational states.

If the carbon dioxide laser is tuned to a different line, one expects to observe a change in the rotational lines that are depleted. Indeed, when the laser is switched to the 10P(14) line, it was found that the $J = 2$ and $J = 3$ states are considerably depleted. Detailed investigations of carbon dioxide laser excitation of several other molecules analyzed by CARS spectroscopy have been published elsewhere.[13]

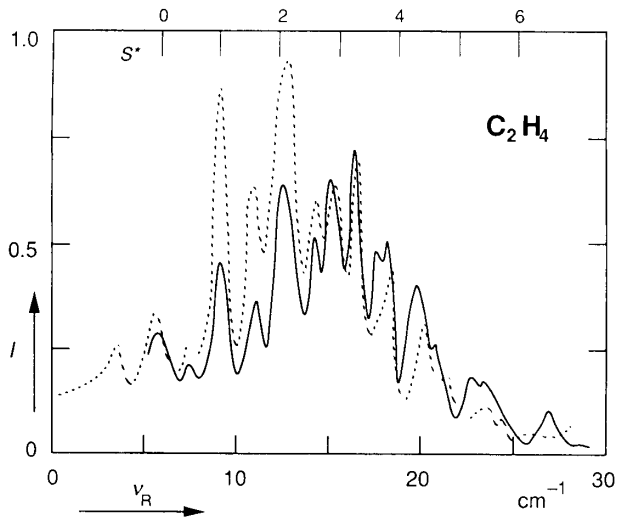

Figure 10. Pure rotational CARS spectra of ethylene in the beam at $x/D = 5.7$, without infrared excitation (dashed line) and 250 ns after 10P(14) carbon dioxide laser excitation (solid line). Note the depletion of the $J = 1$ and $J = 2$ levels.

CONCLUSIONS

A three-dimensional approach for phase matching in pure rotational multiplex CARS measurements with a single broad-band dye laser has been presented. The technique has been applied to study the rotational cooling of nitrogen in a supersonic beam, and the depletion of rotational levels in the infrared multiphoton excitation of ethylene.

For asymmetric top molecules (the majority of polyatomic molecules), the rotational spectra are complicated with many, frequently overlapping, branches. As shown by the data for ethylene, these spectra can still be resolved using the multiplex pure rotational CARS technique presented here. The technique therefore allows the direct observation of laser-induced changes in rotational population. It should also be possible to study the rotational distributions of molecular fragments following laser-induced photodissociation.

It is concluded that the instrumentation is greatly simplified over previous approaches. In fact, it is identical with that for vibrational CARS and therefore it is relatively simple to switch back and forth between vibrational and pure rotational CARS. Since the scheme is independent of the frequency difference between the dye laser and its pump laser, not even a change of dye is required. Since the rotational constants of molecules are all small, only one dye is required to measure different species. This means that one can use this technique to monitor the rotational populations of a number of species simultaneously. The method works extremely well even for Raman shifts as small as a few wavenumbers (see Figs 8–10). Because all photons within the broad-band dye laser profile are used to generate a signal, the methods can be extended to even lower density than the vibrational CARS scheme. Finally, the method permits a more detailed analysis of vibrational excitation by carbon dioxide laser pulses, both in the collisional and collisionless regimes.

Acknowledgements

We acknowledge many useful discussions with Shrenik Deliwala and Jay Goldman. This work was supported by the Army Research Office contracts DAAL03-88-K-0114 and DAAL03-86-G-70098, the Joint Services Electronics Program contract N00014-84-K-0465 and by Hamamatsu Photonics K.K.

REFERENCES

1. J. W. Nibler and G. A. Pubanz, in *Advances in Non-Linear Spectroscopy*, edited by J. H. Clark and R. E. Hester, p. 78. Wiley, Chichester (1988).
2. R. P. Lucht, *Opt. Lett.* **12**, 78 (1987).
3. F. Y. Yueh and E. D. Beiting, *Appl. Opt.* **27**, 3233 (1988).
4. A. C. Eckbreth and T. J. Anderson, *Appl. Opt.* **23**, 1328 (1984).
5. B. Dick and A. Gierulski, *Appl. Phys. B* **40**, 1 (1986).

6. J. B. Zheng, J. B. Snow, D. V. Murphy, A. Leipertz, R. K. Chang and R. L. Farrow, *Opt. Lett.* **9**, 341 (1984).
7. A. C. Eckbreth and T. J. Anderson, *Opt. Lett.* **11**, 496 (1986).
8. J. A. Shirley, R. J. Hall and A. C. Eckbreth, *Opt. Lett.* **5**, 380 (1980).
9. W. B. Roh P. W. Schreiber and J. P. Taran, *Appl. Phys. Lett.* **29**, 174 (1976).
10. W. Fuss and K. L. Kompa, *Prog. Quantum Electron* **7**, 117 (1981).
11. N. Bloembergen and E. Yablonovitz, *Phys. Today* **5**, 23 (1978).
12. D. S. King, in *Dynamics of the Excited State*, edited by K. P. Lawley, Wiley, New York, 1982, p. 105.
13. K. H. Chen, C. Z. Lü, L. A. Avilés, E. Mazur, N. Bloembergen and M. J. Shultz, *J. Chem. Phys.* **91**. 1462 (1989).
14. Y. R. Shen, *The Principles of Nonlinear Optics*. Wiley, New York (1984).
15. G. Placzek and E. Teller, *Z. Physik*, **81**, 209 (1933).
16. J. B. Anderson, *Molecular Beam and Low Density Gas Dynamics*. Marcel Dekker, New York (1974).
17. J. B. Anderson, *AIAA J.* **10**, 111 (1972).
18. P. Huber-Walchli and J. W. Nibler, *J. Chem. Phys.* **76**, 273 (1982).
19. G. Luijks, S. Stolte and J. Reuss, *Chem. Phys.* **62**, 217 (1981).
20. G. Herzberg, *Infrared and Raman Spectra of Polyatomic Molecules*. Van Nostrand, New York (1945).
21. J. Romanko, T. Feldman, E. J. Stansbury and A. McKellar, *Can. J. Phys.* **32**, 375 (1954).
22. G. Herzberg, *Electronic Spectra of Polyatomic Molecules*. Van Nostrand, New York (1966).